Dynamic Performance Control of Modular Multilevel Converters in HVDC Transmission Systems

M. Mehrasa
Babol (Noshirvani) Univ. of Technology, Babol, Iran

S.K. Hosseini and S. Taheri
Université du Québec en Outaouais Gatineau, Canada

E. Pouresmaeil and J.P.S. Catalão
INESC TEC and FEUP, Porto, C-MAST/UBI, Covilha, and INESC-ID/IST-UL, Lisbon, Portugal

***Abstract*—This paper focuses on dynamic performance control of modular multilevel converters (MMC) in high-voltage direct current (HVDC) transmission systems. To achieve this objective, a new mathematical model including six state variables of ac-currents and dc-link voltage of MMC, and circulating currents of converter arms are proposed for MMC in d-q reference frame. In addition, a robust control technique with three sub-control loops is designed to provide the stable operation of MMC. In the overall structure of the proposed controller, three outer, central and inner loops have the duties of 1) making the state variables error zero with changeable convergence rate, 2) adding robustness characteristic to the proposed controller, and 3) generating the appropriate reference values for MMC's currents, respectively. The effectiveness of the proposed control algorithm is investigated via MATLAB simulation. The simulation results highlight the capability of the proposed control algorithm in offering an accurate active and reactive power tracking through the control method of MMC, a stabilized dc-link voltage, capacitor voltage balancing of sub-modules, and minimization of circulating currents of converter arms during dynamic transitions and steady state operation.**

Keywords—Modular multilevel converter (MMC); capacitor voltage balancing; circulating current control.

I. INTRODUCTION

Increasingly, modular multilevel converter (MMC) topology is frequently being used since it offers distinguished features such as distributed (decentralized) energy storages, modular structure, easy redundant sub-modules (SMs), simple fault identification and clearance, common dc-bus and other characteristics of less power losses, low rating components, and a more effective reduction of harmonic contents [1]-[5].

Over the past few years, significant studies have been done to address the different challenges associated with the operation and control of the MMCs as well as broadening its applications. In [6], an energy-balancing control strategy has been proposed aiming normal operation of MMC under fault conditions. A model predictive control (MPC) strategy has been proposed in [7] for an MMC-based back-to-back HVDC system in order to minimize the circulating currents of MMC arms and to balance its capacitor voltages. A methodology is proposed in [8] for a MMC-based HVDC system to achieve desired operative conditions by calculating the differential current references. These reference currents are established through a number of constraints in the formulation of optimization problems that leaded to the minimized oscillations of differential current and capacitive phase-energy.

This paper aims to present a robust control technique for stable operation of back-to-back MMCs in HVDC transmission system. The main contributions of the paper can be stated as: 1) a new dynamic model of MMC in d-q reference frame with six state variables including MMC's currents, dc-link voltage, and circulating currents of converter arms, 2) a robust controller consisting of three sub-loops with the duties of making the state variables error zero with changeable convergence rate, adding robustness characteristic to the proposed controller, and generating the appropriate reference values for MMC's currents, respectively. The efficiency and applicability of the proposed control technique are verified through several systematic numerical simulations, implemented in MATLAB.

II. THE DYNAMIC MODEL FOR AN MMC-BASED HVDC SYSTEM

A general schematic diagram of the proposed model is illustrated in Fig.1. The proposed model is composed of two MMCs, in which MMC1 is a rectifier whereas MMC2 operates as an inverter. The dc-link is responsible to transfer the generated dc power via MMC1 into MMC2. Resistor R_{dc} connected in parallel with the dc-link, reflects total switching loss of the HVDC converter stations. Each converter consists of six arms, an inductor and a resistor. Each SM operates as a half-bridge converter with two complement switches with a freewheeling diode. Arm inductors are used to suppress the circulating current and also to limit fault current during a dc-side fault. The series resistor of each arm represents the combination of the arm losses and inner inductor resistance.

A. Dynamic model of the proposed MMC-based HVDC

As shown in Fig. 1, the dc-link voltage v_{dc} of the proposed back-back MMC is dependent on the sum of the capacitor voltages in both lower and upper arms. Therefore, the dc-link voltage can be accurately regulated by controlling $v_{(ul)kj}$. By applying Kirchhoff's voltage law (KVL) to the Fig. 1, considering the loops with input or output ac voltages of MMCs, the voltage across the lower or upper arm, and the dc-link voltage with virtual neutral midpoint components, the mathematical equations, governing dynamic behavior of the MMCs can be expressed as,

$$v_{kj} + L\frac{di_{kj}}{dt} + Ri_{kj} + L_p\frac{di_{ukj}}{dt} + R_p i_{ukj} - \frac{v_{dc}}{2} + v_{ukj} = 0 \qquad (1)$$

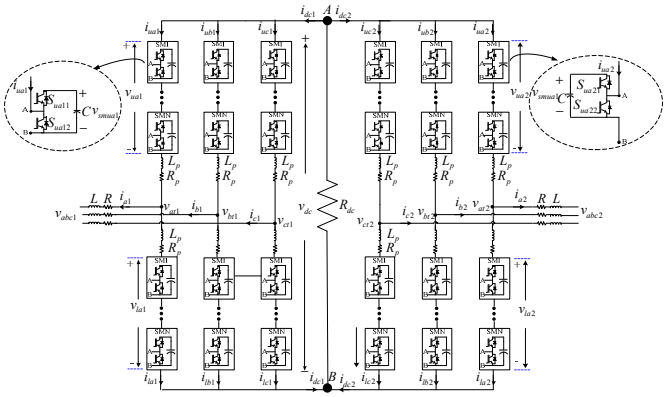

Fig. 1. Schematic diagram of the back-to-back MMC-HVDC system.

$$v_{kj} + L\frac{di_{kj}}{dt} + Ri_{kj} - L_p\frac{di_{lkj}}{dt} - R_p i_{lkj} + \frac{v_{dc}}{2} - v_{lkj} = 0 \tag{2}$$

where j=1, 2. v_{kj} and v_{ulj} are the output and sub-modules voltages of MMCs, i_{kj} and i_{ulj} are output and arms currents of MMCs. Also $\{R, L\}$ and $\{R_p, L_p\}$ are related to the output and arm's parameters of MMCs. By summation of (1) and (2), a dynamic model can be achieved based on the input or output currents of MMCs as,

$$\left(L + 0.5L_p\right)\frac{di_{kj}}{dt} + \left(R + 0.5R_p\right)i_{kj} + v_{kj} + u_{kj1} = 0 \tag{3}$$

where $u_{kj1} = 0.5\left(v_{ukj} - v_{lkj}\right)$. u_{kj1} is used to control the MMCs currents to accurately track reference active and reactive power, to reach the desired level of dc-link voltage, and to balance the voltage of SM capacitors in both steady state and dynamic operation conditions, and during parameter variation transitions. The MMCs suffers from the presense of currents circulating within the three phases which cuase an increment in the MMCs losses, in capacitor voltage ripple magnitude, as well as in cost of the MMCs. An attempt is made in this work to reduce the circulating currents.

According to the Fig. 1, the circulating current can be expressed as $i_{cirkj} = \left(i_{ukj} + i_{lkj}\right)/2 - i_{dcj}/3$ that i_{dcj} is the dc-link current of MMCs. In order to minimize the circulating currents, the following dynamic model which is based on the circulating currents can be derived from Eq. (1) and (2). Subtracting (1) from (2) gives,

$$L_p\frac{di_{cirkj}}{dt} + R_p i_{cirkj} + R_p\frac{i_{dcj}}{3} - 0.5v_{dc} + u_{kj2} = 0 \tag{4}$$

where, $u_{kj2} = 0.5\left(v_{ukj} + v_{lkj}\right)$. Dynamic equation of the dc-link voltage in the proposed HVDC system can be calculated by applying the Kirchhoff's current law (KCL) to the points A and B in Fig. 1 as follows,

$$C_{eq}\frac{dv_{dc}}{dt} + \frac{v_{dc}}{R_{dc}} + \sum_{k=a}^{b,c} i_{uk1} + \sum_{k=a}^{b,c} i_{uk2} = 0 \tag{5}$$

$$C_{eq}\frac{dv_{dc}}{dt} + \frac{v_{dc}}{R_{dc}} + \sum_{k=a}^{b,c} i_{lk1} + \sum_{k=a}^{b,c} i_{lk2} = 0 \tag{6}$$

The relationship between the dc-link voltage and circulating currents can be obtained by summation of (5) and (6) as,

$$C_{eq}\frac{dv_{dc}}{dt} + \frac{v_{dc}}{R_{dc}} + \sum_{k=a}^{b,c} i_{cirkj} + i_{dc1} + i_{dc2} = 0 \tag{7}$$

Using Park transformation for (3), (4), and (7), results in the dynamic model of the proposed HVDC system in the d-q frame as below,

$$\left(L + 0.5L_p\right)\left(di_{dj}/dt\right) + \left(R + 0.5R_p\right)i_{dj} - \omega\left(L + 0.5L_p\right)i_{qj} + u_{dj1} + v_{dj} = 0 \tag{8}$$

$$\left(L + 0.5L_p\right)\frac{di_{qj}}{dt} + \left(R + 0.5R_p\right)i_{qj} + \omega\left(L + 0.5L_p\right)i_{dj} + u_{qj1} + v_{qj} = 0 \tag{9}$$

$$L_p\frac{di_{cirdj}}{dt} + R_p i_{cirdj} - \omega L_p i_{cirqj} + u_{dj2} = 0 \tag{10}$$

$$L_p\frac{di_{cirqj}}{dt} + R_p i_{cirqj} + \omega L_p i_{cirdj} + u_{qj2} = 0 \tag{11}$$

$$L_p\frac{di_{cir0j}}{dt} + R_p i_{cir0j} + u_{0j2} - \frac{3\sqrt{2}v_{dc}}{2} + \sqrt{2}R_p i_{dcj} = 0 \tag{12}$$

$$C_{eq}\frac{dv_{dc}}{dt} + \frac{v_{dc}}{R_{dc}} + \sqrt{3}i_{cir0j} + i_{dc1} + i_{dc2} = 0 \tag{13}$$

C_{eq} is the equivalent capacitance of MMCs sub-modules. Equations (8)-(13) are used to design the proposed control technique, to analyze the power conversion of MMCs, and stability analyzes of the proposed model.

III. Control Discussion

The proposed control technique in this paper consists of three loops as Outer Loop Controller (OLC), Central Loop Controller (CLC), and Inner Loop Controller (ILC). OLC is designed in order to conduct the dynamic errors to reach the zero value by injection of series resistance to the resultant dynamic equations and also by energy shaping.

CLC is designed to support stable behavior for the proposed MMC-based HVDC system against the parameter variation. The last part of the proposed controller is ILC, which is schemed to create accurate reference currents for both MMC1 and MMC2 with respect to the control aims of each converter.

Contribution of all three sub-control loops to the overall control scheme promotes the proposed MMCs performance to reach an accurate active and reactive power tracking, a desired level of dc-link voltage, a minimized circulating current in the converter arms, and a balanced voltage for the SM capacitors. Sub-controller features are discussed in the following sub-sections in details.

A. OLC for the MMCs

A close loop control algorithm is required for MMCs to appropriately track reference current components during the deviations of state variables from its desired values and the error of dynamic changes. To achieve this goal, the matrix representation of dynamic model of MMCs in (8)-(13) can be expressed as,

$$T_{dq0j}\frac{dQ_{dq0j}}{dt} + X_{dq0j}Q_{dq0j} + P_{dq0j} + O_{dq0j} + Y_{dq0j} = 0 \tag{14}$$

Details of the matrixes in (14) are given in the following.

$$Q_{dq0j}=\begin{bmatrix} i_{dj} & i_{qj} & i_{cirdj} & i_{cirqj} & i_{cir0j} & v_{dc}\end{bmatrix}^T$$

$$P_{dq0j}=\begin{bmatrix} u_{dj1} & u_{qj1} & u_{dj2} & u_{qj2} & u_{0j2} & 0\end{bmatrix}^T$$

$$O_{dq0j}=\begin{bmatrix} 0 & 0 & 0 & 0 & \sqrt{2}R_p i_{dcj} & i_{dc1}+i_{dc2}\end{bmatrix}^T$$

$$Y_{dq0j}=O_{dq0j}=\begin{bmatrix} v_{dj} & v_{qj} & 0 & 0 & 0 & 0\end{bmatrix}^T$$

$$T_{dq0j}=\begin{bmatrix} R+0.5R_p & 0 & 0 & 0 & 0 & 0\\ 0 & R+0.5R_p & 0 & 0 & 0 & 0\\ 0 & 0 & L_p & 0 & 0 & 0\\ 0 & 0 & 0 & L_p & 0 & 0\\ 0 & 0 & 0 & 0 & L_p & 0\\ 0 & 0 & 0 & 0 & 0 & C_{eq}\end{bmatrix}$$

$$X_{dq0j}=\begin{bmatrix} (R+0.5R_p) & -\omega(L+0.5L_p) & 0 & 0 & 0 & 0\\ \omega(L+0.5L_p) & (R+0.5R_p) & 0 & 0 & 0 & 0\\ 0 & 0 & R_p & -\omega L_p & 0 & 0\\ 0 & 0 & \omega L_p & R_p & 0 & 0\\ 0 & 0 & 0 & 0 & R_p & -\frac{3\sqrt{2}}{2}\\ 0 & 0 & & 0 & \sqrt{3} & \frac{1}{R_{dc}}\end{bmatrix}$$

The vectors of the tracking errors for the proposed model can be expressed as,

$$Z_{dq0j}=Q_{dq0j}-Q^*_{dq0j}= \tag{15}$$

$$\begin{bmatrix} i_{dj}-i^*_{dj} & i_{qj}-i^*_{qj} & i_{cirdj}-i^*_{cirdj} & i_{cirqj}-i^*_{cirqj} & i_{cir0j}-i^*_{cir0j} & v_{dc}-v^*_{dc}\end{bmatrix}^T$$

The reference values in (15) are obtained based on accurate power sharing of the MMCs and the regulation of dc and ac output voltages.

Dynamic model of the closed-loop error of the proposed HVDC system is extracted from the combination of (14) and (15) as,

$$\begin{aligned} &T_{dq0j}\frac{dZ_{dq0j}}{dt}+X_{dq0j}Z_{dq0j}=\\ &-Q_{dq0j}-Y_{dq0j}-P_{dq0j}-\left(T_{dq0j}\frac{dQ^*_{dq0j}}{dt}+X_{dq0j}Q^*_{dq0j}\right)\end{aligned} \tag{16}$$

Equation (16) can be modified in order to reach a faster convergence of error variables to zero in OLC. This can be achieved by injection of series resistances in the error dynamic model of the proposed HVDC model. The series resistance matrix for MMCs is given in (17),

$$R_{dq0j}=\begin{bmatrix} R_d & 0 & 0 & 0 & 0 & 0\\ 0 & R_q & 0 & 0 & 0 & 0\\ 0 & 0 & R_{cird} & 0 & 0 & 0\\ 0 & 0 & 0 & R_{cirq} & 0 & 0\\ 0 & 0 & 0 & 0 & R_{cir0} & 0\\ 0 & 0 & 0 & 0 & 0 & (R_{dc})^{-1}\end{bmatrix}$$

By adding $R_{dq0j}Z_{dq0j}$, the passive-injection term into the both sides of (16), the modified dynamic model of the closed-loop error of the proposed HVDC system can be derived as,

$$\begin{aligned} &T_{dq0j}\frac{dZ_{dq0j}}{dt}+X_{dq0j}Z_{dq0j}+R_{dq0j}Z_{dq0j}=\\ &-Q_{dq0j}-Y_{dq0j}-P_{dq0j}-\left(T_{dq0j}\frac{dQ^*_{dq0j}}{dt}+X_{dq0j}Q^*_{dq0j}-R_{dq0j}Z_{dq0j}\right)\end{aligned} \tag{18}$$

All objectives of the OLC for the fast tracking of the reference values in the steady state and/or during presence of load changes are properly attained by $Z_{dq0j}\to 0$; therefore,

$$T_{dq0j}\frac{dZ_{dq0j}}{dt}+X_{dq0j}Z_{dq0j}+R_{dq0j}Z_{dq0j}=0 \tag{19}$$

The proposed dynamic model of OLC, based on the reference signals and error state variables are derived by substituting (19) into (18),

$$\begin{aligned} &-Q_{dq0j}-Y_{dq0j}-P_{dq0j}\\ &-\left(T_{dq0j}\frac{dQ^*_{dq0j}}{dt}+X_{dq0j}Q^*_{dq0j}-R_{dq0j}Z_{dq0j}\right)=0\end{aligned} \tag{20}$$

The designed OLC obtained through the dynamic model of (20) can guarantee zero value for the error state variables as (19) is taken into account to derive it. Therefore, the equivalent modulation functions of converters in OLC can be achieved as,

$$\begin{aligned} &P_{dq0j}=\\ &\left[-Q_{dq0j}-Y_{dq0j}-\left(T_{dq0j}\frac{dQ^*_{dq0j}}{dt}+X_{dq0j}Q^*_{dq0j}-R_{dq0j}Z_{dq0j}\right)\right]\end{aligned} \tag{21}$$

The stability of the proposed error dynamic model and OLC is investigated through the direct Lyapunov method (DLM). The total saved energy of the proposed HVDC system can be presented as (22),

$$\begin{aligned} &E_{dq0j}\left(Z_{dq0j}\right)=\frac{1}{2}\left(L+0.5L_p\right)\left(z_{dj}\right)^2+\\ &\frac{1}{2}\left(L+0.5L_p\right)\left(z_{qj}\right)^2+\frac{1}{2}L_p\left(z_{cirdj}\right)^2+\frac{1}{2}L_p\left(z_{cirqj}\right)^2\\ &+\frac{1}{2}L_p\left(z_{cir0j}\right)^2+\frac{1}{2}C_{eq}\left(z_{dc}\right)^2\end{aligned} \tag{22}$$

where, z=x-x* specifies the difference between reference and measured values in 0dq frame. In order to compensate disturbances to achieve the proposed systems stability, following conditions should be fulfilled i.e. positive total saved energy and a negative derivative of the defined Lyapunov function candidate in whole the system in the state variables trajectories Derivative of the saved energy function in the direction of the error state variables can be obtained as,

$$\begin{aligned} &\frac{dE_{dq0j}}{dt}\left(Z_{dq0j}\right)=\left(L+0.5L_p\right)\frac{dz_{dj}}{dt}z_{dj}+\\ &\left(L+0.5L_p\right)\frac{dz_{qj}}{dt}z_{qj}+L_p\frac{dz_{cirdj}}{dt}z_{cirdj}+L_p\frac{dz_{cirqj}}{dt}z_{cirqj}\\ &+L_p\frac{dz_{cir0j}}{dt}z_{cir0j}+C_{eq}\frac{dz_{dc}}{dt}z_{dc}=T_{dq0j}\frac{dZ_{dq0j}}{dt}Z_{dq0j}\\ &=-\left(X_{dq0j}Z_{dq0j}+R_{dq0j}Z_{dq0j}\right)Z_{dq0j}\end{aligned} \tag{23}$$

Considering (19) in evaluation of (23), it is turned out that terms affected by the injection resistances are more dominant than other terms; therefore, (23) can be rewritten as,

$$\frac{dE_{dq0j}}{dt}\left(Z_{dq0j}\right)=-R_{dq0j}Z_{dq0j}Z_{dq0j}= \\ -R_{dj}\left(z_{dj}\right)^2-R_{qj}\left(z_{qj}\right)^2-R_{cirdj}\left(z_{cirdj}\right)^2-R_{cirqj}\left(z_{cirqj}\right)^2 \\ -R_{cir0j}\left(z_{cir0j}\right)^2-\left(R_{dcj}\right)^{-1}\left(z_{dcj}\right)^2<0 \tag{24}$$

Equation (24) confirms that the OLC based on the proposed dynamic model of the closed-loop error is globally asymptotically stable. The overall structure of OLC for both MMC1 and MMC2 is depicted in Fig. 2, where the decoupled control strategies for the currents of MMCs and circulating currents can be seen. Fig. 2(a) indicates the control strategy for currents of MMCs in order to regulate the power sharing of MMCs in dynamic and steady state operating conditions. Fig. 2(b) shows the technique adopted for minimizing circulating currents in dynamic and steady state operating conditions.

B. CLC for the MMCs

The central part of the proposed controller comprises the sliding-mode controller designed to maintain dc-link voltage, SMs, and ac output voltages at its desired values, in spite of parameters variations. A time-varying sliding surface for MMCs is defined as,

$$S_{dq0j}\left(t,Z_{dq0j}\right)=\left(\frac{d}{dt}+k_{dq0j}\right)^{g_n-1}Z_{dq0j} \tag{25}$$

where, k_{dq0j} can assist state variables on the sliding surface to converge faster. In this section, dynamics of the reference values in the control loop of the MMCs and circulating currents proportional to the defined sliding surface are modified based on the proposed dynamic model of the closed-loop error. By considering (25) and the relative degree 1 for i_{dqj} and $i_{cirdq0j}$, the desired sliding surfaces of the currents of MMCs and circulating currents in d and q-axis can be obtained as,

$$S_{dqj1}\left(t,\mathrm{z}_{dqj}\right)=z_{\mathrm{dqj}}=i_{dqj}-i^*_{dqj} \tag{26}$$

$$S_{dq0j2}\left(t,\mathrm{z}_{cirdq0j}\right)=z_{cir(dq0)j}=i_{cir(dq0)j}-i^*_{cir(dq0)j} \tag{27}$$

The first-order dynamic of achieved sliding surface for each state variable is calculated to motivate the system to move on the sliding surface and track the motion of the state variables on the sliding surface. Therefore, the sign function is employed to make suitable sliding surfaces as,

$$\frac{dz_{(dq)j}}{dt}=\frac{di_{(dq)j}}{dt}-\frac{di^*_{(dq)j}}{dt}=-\psi_{(dq)j}\,\mathrm{sgn}\left(z_{(dq)j}\right) \tag{28}$$

$$\frac{dz_{cir(dq0)j}}{dt}=\frac{di_{cir(dq0)j}}{dt}-\frac{di^*_{cir(dq0)j}}{dt}=-\psi_{cir(dq0)j}\,\mathrm{sgn}\left(z_{cir(dq0)j}\right) \tag{29}$$

Through a proper selection of $\psi_{(dq)j}$ and $\psi_{cir(dq0)j}$, the converging speed and tracking capability of the designed CLC will be significantly improved.

Fig. 3 shows the entire design process of the proposed CLC for the control of currents of MMCs and circulating currents under parameter variation condition in the proposed HVDC model.

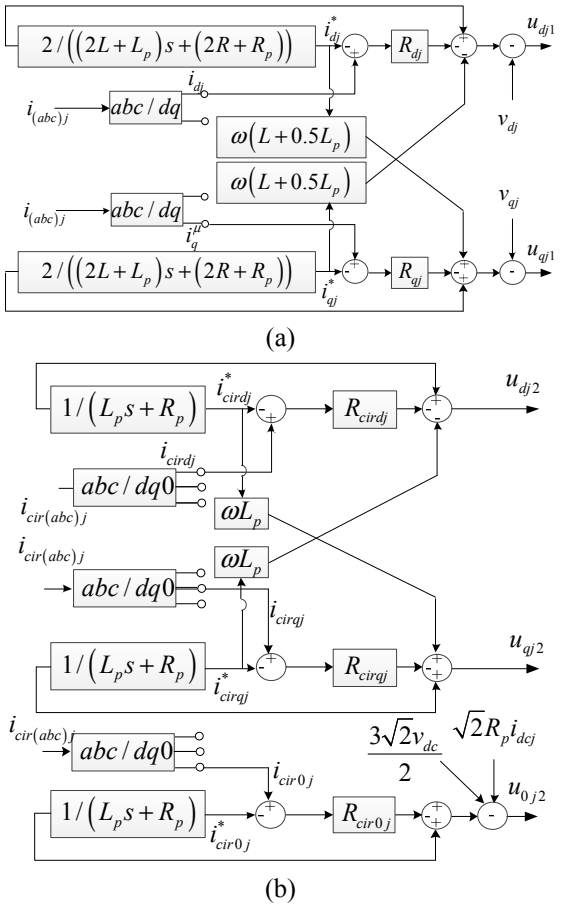

Fig. 2. Overall structure of the OLC for both MMC1 and MMC2 in the proposed HVDC system. (a) OLC for the MMCs currents control and (b) OLC for the MMCs circulating currents control.

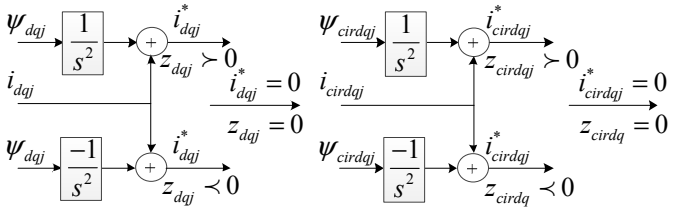

Fig. 3. The overall structure of CLC for both MMCs. (a) CLC for the control of the currents of MMCs and (b) CLC for the control of circulating currents of MMCs.

A symmetric operation in CLC for both MMCs and circulating currents can be seen in figure 3. The stability of the proposed CLC is evaluated by DLM. Therefore, the Lyapunov function of the proposed system based on the sliding surfaces can be expressed as,

$$J_j(Q)=\frac{1}{2}\left(z_{dj}\right)^2+\frac{1}{2}\left(z_{qj}\right)^2+\frac{1}{2}\left(z_{cirdj}\right)^2+\frac{1}{2}\left(z_{cirqj}\right)^2+\frac{1}{2}\left(z_{cir0j}\right)^2 \tag{30}$$

By derivative of (30) along the state variables trajectories, (31) can be obtained as,

$$\frac{dJ_j(Q)}{dt}=z_{dj}\frac{dz_{dj}}{dt}+z_{qj}\frac{dz_{qj}}{dt}+z_{cirdj}\frac{dz_{cirdj}}{dt}+z_{cirqj}\frac{dz_{cirqj}}{dt}+ \\ z_{cir0j}\frac{dz_{cir0j}}{dt}=-z_{dj}\psi_{dj}\,\mathrm{sgn}\left(z_{dj}\right)-z_{qj}\psi_{qj}\,\mathrm{sgn}\left(z_{qj}\right)-z_{cirdj}\psi_{cirdj}\times \\ \mathrm{sgn}\left(z_{cirdj}\right)-z_{cirqj}\psi_{cirqj}\,\mathrm{sgn}\left(z_{cirqj}\right)-z_{cir0j}\psi_{cir0j}\,\mathrm{sgn}\left(z_{cir0j}\right)\le 0 \tag{31}$$

Equation (31) should have a negative value to meet the stability criteria during operation of MMCs in the proposed model. To reach this goal, all the terms in (31) should be analyzed properly. By considering the definition of the sgn-function, the term $z_{xj}\,\mathrm{sgn}\left(z_{xj}\right)$ is always positive or zero. As a result of minus multiplication to all available terms, the whole combination has negative or zero value. Therefore, application of DLM technique can guarantee a stable operation for the proposed sliding mode controller during both dynamic and steady state operational conditions.

C. ILC for the MMCs

Assuming that connected loads in the proposed model are nonlinear with low harmonic components, fundamental and harmonic components of the load should be supplied only through the MMC2. Total harmonic components of the load current are separated from the fundamental frequency as follows

$$\sum_{h=1}^{\infty} i_{l(dq)h} = i_{l(dq)}\left(1-\frac{\omega_{(dq)2}}{s+\omega_{(dq)2}}\right) \tag{32}$$

The applied transfer function in (32) is a type of low pass filter (LPF) which allows an extraction of the harmonic frequencies of current from the main frequency of load current. On the other hand, MMC2 is regulated to generate active and reactive power in fundamental frequency.

General structure of the proposed ILC for MMC2 is shown in Fig. 4(a), including aforementioned mechanisms and using suitable PI controllers. The cut-off frequency of LPF and PI controller gains requires to be calculated precisely in order to reach the desired reference currents for MMC2. This concept will be discussed in the next section. Fig. 4(b) shows the swinging components of the dc-link voltage, which are used to generate the reference current values in d and q-axis for MMC1. Q_{l2} is the total reactive power of loads connected to the ac side of MMC1.

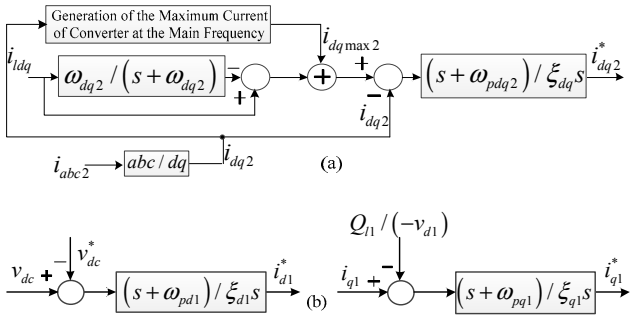

Fig. 4. The overall structure of ILC for both MMCs. (a) ILC for the reference currents of MMC2 and (b) ILC for the reference currents of MMC1.

IV. Results And Discussion

To demonstrate the performance of proposed control technique in the control and operation of the MMCs in the HVDC transmission systems the proposed MMC-HVDC is modeled in the Matlab/Simulink environment. The system parameters are given as Table I.

TABLE I
SIMULATION PARAMETERS

f_{ac}	60 Hz	n	3
f_s	10 kHz	C	25mF
v_{dc}	42kV	C_{fi}	615µF
v_c	14kV	P_j	150MW
L_{jk}	25mH	Q_j	75MVAR
R_{jk}	1Ω	MMC1 load I	65MW,-20MVAR
L_k	6mH	MMC2 load I	20MW,7MVAR
R_k	0.3Ω		

A. Evaluation of proposed model response to the parameter variation

To evaluate the performance of the proposed CLC controller when resistances and inductances change, a pattern of mentioned paremerts change as shown in Fig. 5 is considered. On the other hand, the OLC is utilized for controlling the MMC-based HVDC system in steady state operation in the first step of simulation. Fig. 6 shows the system's dc-link voltage and the SM capacitor voltages in both MMCs. As indicated in this figure, by using the CLC in the proposed control technique, the parameter change has no impact on the dc-link voltage except for negligible ripples in a short transient time. In addition, the ripples on SM capacitor voltages are slightly increased after a change in parameters, however the voltages eventually reach their steady state value at $v_{dc}/3$.

Fig. 7 confirms that, the ac-sides of MMCs are able to provide the balance three phase voltages during the parameter variation.

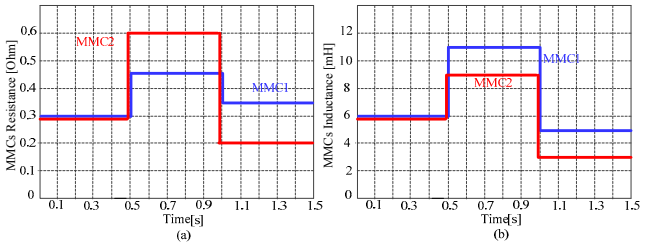

Fig. 5. Resistance and inductance variations of MMCs. (a) MMCs resistance variations and (b) MMCs inductance variations.

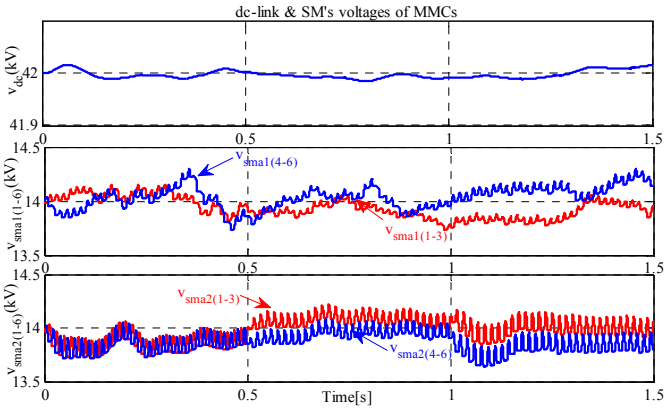

Fig. 6. dc-link and SM's voltages of MMCs under the parameters variations.

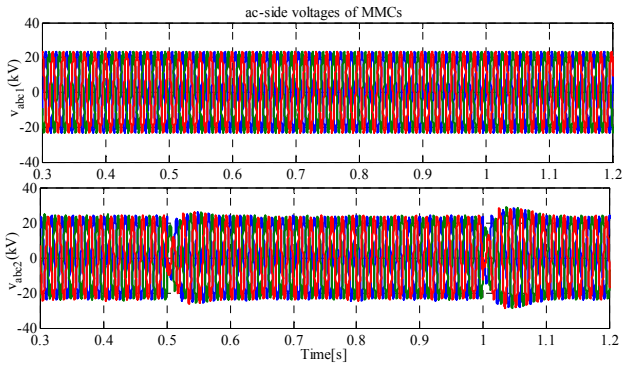

Fig. 7. ac voltages of MMCs under the parameters variations.

Furthermore, minimizing circulating currents task is accurately executed in this process. The circulating currents are effected by parameter variation, particularly at t=1.1sec as shown in Fig. 8. However, dynamic performance of the CLC reduces slightly the negative impacts due to parameter variations and the MMCs circulating currents are noticeably minimized into a desirable level.

In this section, the active and reactive power of 140MW+j45MVAR and 35MW+j25MVAR are considered for the ac-side of MMC1 and MMC2, respectively as shown in Fig. 9. As can be seen, the first step of parameters changes leads to a decrease in the active power and an increase in the reactive power due to a resistance decrement and a reactance increment. In the second step of parameters changes, active and reactive power of MMC1 demonstrates a reverse operation toward the first step of variation.

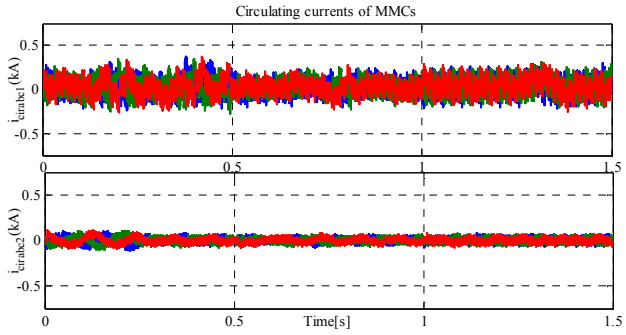

Fig. 8. Circulating currents of MMCs under the parameters variations.

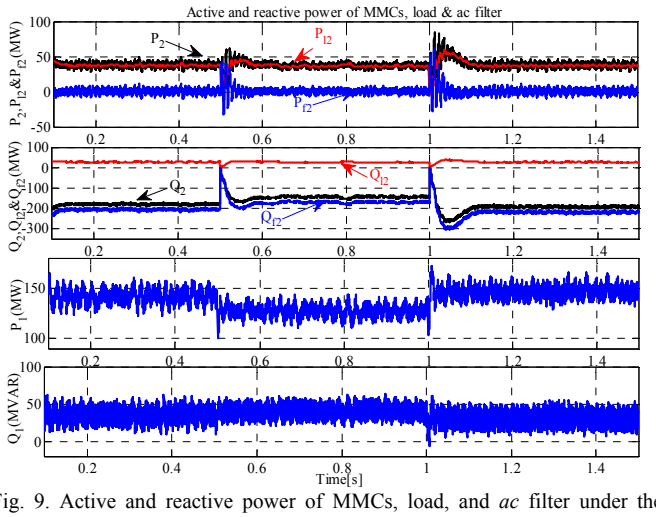

Fig. 9. Active and reactive power of MMCs, load, and *ac* filter under the parameters variations.

Thus, despite of parameters variations for MMC2, a fast power tracking is accomplished by the CLC in MMC2. The injected reactive power of ac filter is changed proportionally to keep the output voltages at desired value.

V. Conclusion

A robust control technique was presented in this paper for control of a back-to-back VSC-HVDC system based on the MMC converter. The overall dynamic model of the proposed MMC-based HVDC system was thoroughly investigated and three sub-controllers (OLC, CLC, and ILC) were proposed for the control of the MMCs under different operating conditions. Moreover, a power curve was achieved to evaluate better the active and reactive power operation of MMC. The proposed model was implemented in time-domain using Matlab/Simulink environment. The simulation results indicated that the proposed control technique is able to guarantee a stable operation for the MMCs with a fast dynamic response to any changes in the system parameters. In addition, the proposed control technique can effectively provide voltage balancing for the capacitor of the sub-modules under the dynamic and steady state operating conditions, i.e., under the step load increment and system parameters variations. Furthermore, the proposed control technique provides the desired dc-link voltage for the system and minimizes circulating currents of converter arms.

Acknowledgement

This work was supported by FEDER funds (European Union) through COMPETE, and by Portuguese funds through FCT, under Projects FCOMP-01-0124-FEDER-020282 (Ref. PTDC/EEA-EEL/118519/2010), UID/CEC/50021/2013 and SFRH/BPD/102744/2014. Also, the research leading to these results received funding from the EU Seventh Framework Programme FP7/2007–2013 under grant agreement no. 309048. Moreover, the authors would like to thank Natural Sciences and Engineering Research Council of Canada (NSERC) for financial support which made this research possible.

References

[1] A. Lesnicar and R. Marquardt, “An innovative modular multilevel converter topology suitable for a wide power range,” in *Proc. 2003 IEEE Power Tech Conf*., Bologna, Italy, 2003.

[2] S. Fan, K. Zhang, J. Xiong, and Y. Xue, “An Improved Control System for Modular Multilevel Converters with New Modulation Strategy and Voltage Balancing Control,” *IEEE Trans. Power Electron*., vol. 30, no. 1, pp. 358 - 371, Feb. 2014.

[3] E. Pouresmaeil, M. Mehrasa, M.A Shokridehaki, E.M.G Rodrigues, and J.P.S Catalão, “Control of Modular Multilevel Converters for Integration of Distributed Generation Sources into the Power Grid,” *International Conference on Smart Energy Grid Engineering (SEGE)* 2015; 1-6.

[4] L. Harnefors, A. Antonopoulos, S. Norrga, L. Angquist, and H-P Nee, “Dynamic Analysis of Modular Multilevel Converters,” *IEEE Trans. Industrial Electron*., vol. 60, no. 7, pp. 2526-2537, Jul. 2013.

[5] K. Ilves, A. Antonopoulos, S. Norrga, and H.-P. Nee, “Steady-state analysis of interaction between harmonic components of arm and line quantities of modular multilevel converters,” *IEEE Trans. Power Electron*., vol. 27, no. 1, pp. 57-68, Jan. 2012.

[6] S. Debnath, Q. Jiangchao, B. Bahrani, M. Saeedifard, and P. Barbosa, “Operation, Control, and Applications of the Modular Multilevel Converter: A Review,” *IEEE Trans. Power Electron.*, vol. 30, no. 1, pp. 37 - 53, March. 2014.

[7] P. Hu, D. Jiang, Y. Zhou, Y. Liang, J. Guo, and Z. Lin, “Energy-balancing Control Strategy for Modular Multilevel Converters Under Submodule Fault Conditions,” *IEEE Trans. Power Electron.*, vol. 29, no. 9, pp. 5021 - 5030, Sep. 2014.

[8] Q. Jiangchao and M. Saeedifard, “Predictive Control of a Modular Multilevel Converter for a Back-to-Back HVDC System,” *IEEE Trans. Power Delivery*., vol. 27, no. 3, pp. 1538 - 1547, Apr. 2012.